ALKALI EARTH METAL INDATES SYNTHESIZED BY PRECURSOR METHOD

D. GINGASU[a], O. OPREA[b,*], I. MINDRU[b], D. C. CULITA[a], L. PATRON[a]
[a]*"Ilie Murgulescu" Institute of Physical Chemistry of Romanian Academy, Splaiul Independentei 202, 060021 Bucharest, Romania*
[b]*"Politehnica" University of Bucharest, Faculty of Chemistry, Polizu Street, no. 1-7, Bucharest, Romania*

Precursor method was used in order to obtain alkali earth metal indates. The multimetallic complexes, namely: $(NH_4)_4[CaIn_2(C_4O_6H_4)_3(OH)_6]\cdot 4H_2O$, $(NH_4)_3[SrIn_2(C_4O_6H_4)_3(OH)_5]\cdot 4H_2O$ and $(NH_4)_3[BaIn_2(C_4O_6H_4)_3(OH)_5]\cdot 3H_2O$ have been synthesized and investigated by infrared and emission spectra as well as by thermal analysis. The alkali earth metal indates obtained by decomposition of these compounds have been characterized by X-ray powder diffraction, infrared, diffuse reflectance and emission spectra. The photocatalytic activity was evaluated.

(Received June 21, 2011; accepted August 24, 2011)

Keywords: Nanoparticles; Alkali earth metal indates; Precursor method; X-ray diffraction

1. Introduction

Semiconductor photocatalysts have been the target of many investigations because of their applications in the areas of solar energy, water splitting and air and wastewater purification [1-5].

In the last decade, Inoue and Zou et al. have demonstrated that p-block metal oxides of MIn_2O_4 type (M^{2+} = Ca^{2+}, Sr^{2+}, Ba^{2+}) have good photocatalytic activity for degrading organic pollutants like methylene blue (MB) under visible light or water-splitting into hydrogen and oxygen [1-3].

The most common method for preparing of these materials is the solid-state reaction (SSR) of the component oxides (known as the ceramic method). However, this procedure requires high reaction temperatures/long time treatments and produces particles with large size and a limited degree of homogeneity [6]. For this reason, wet chemical methods like coprecipitation [5], solution-combustion (SC) method using urea/glycine as fuels [7-9] are preferred. Another procedure belonging to the chemical methods is the so-called „complexation method" based on the thermal or *in situ* decomposition of the multimetallic precursor [10-12]. This method requires:

- a detailed study of the parameters (the nature of the ligand, the M^{n+}:L ratio, the pH of reaction medium, the temperature, etc.) influencing the synthesis of the multimetallic complex compounds;
- a study about the thermal decomposition of the complex compound precursors in order to establish the temperature formation of the mixed oxides, followed by the characterization of these oxides.

The selection of the ligand is the most important stage in this procedure because it is necessary to obtain complex compounds that can be easily decomposed at low temperatures, with the formation of volatile products. From this viewpoint, the multimetallic compounds containing tartarate anions as ligands are strongly recommended [13-15].

The aim of this work was the preparation of alkali earth metal indates by thermal decomposition of multimetallic tartarate compounds (the complexation method, named, also, the precursor method).

* Corresponding author: ovidiu73@yahoo.com

2. Experimental

2.1. Synthesis of the tartarate precursors

The following systems have been studied:

$2In^{3+} : 1M^{2+} : 4C_4O_6H_4^{2-}$ where $M^{2+} = Ca^{2+}$, Sr^{2+}, Ba^{2+} and $C_4O_6H_4^{2-}$ = tartarate anion

All chemicals: $In(NO_3)_3 \cdot 5H_2O$, $CaCO_3$, $Sr(NO_3)_2$, $Ba(NO_3)_2$, tartaric acid ($C_4O_6H_6$) were of reagent quality (Merck).

Indium nitrate and alkaline earth (calcium/strontium/barium) salt were dissolved in minimum amount of distilled water and mixed under continuous stirring with an aqueous solution of tartarate acid in a 2:1:4 ratio. Ethanol was added to the final solution until a white precipitate was formed. The pH was raised to 6 by adding NH_4OH:ethanol (1:1). After 24 hours at 4 °C, the precipitate was filtered and dried over P_4O_{10}.

Elemental chemical analysis was consistent with the formula:

$(NH_4)_4[CaIn_2(C_4O_6H_4)_3(OH)_6] \cdot 4H_2O$ ***(I)***: Anal. calcd. % In 23.93; Ca 4.17; C 15.00; N 5.83; H 4.37; found %: In 23.81; Ca 4.50; C 15.30; N 5.76; H 3.65.

$(NH_4)_3[SrIn_2(C_4O_6H_4)_3(OH)_5] \cdot 4H_2O$ ***(II)***: Anal. calcd. % In 23.52; Sr 9.01; C 14.81; N 4.32; H 3.80; found % In 23.52; Sr 8.97; C 15,33; N 4.51; H 3.31.

$(NH_4)_3[BaIn_2(C_4O_6H_4)_3(OH)_5] \cdot 3H_2O$ ***(III)***: Anal. calcd. % In 22.87; Ba13.68; C 14.34; N 4.18; H 3.49; found %: In 22.88; Ba 13.68; C 14.77; N 3.93; H 3.60.

2.2. Physical measurements

The metal content of the tartarate compounds was determined by atomic absorption spectroscopy with a SAA1 instrument and by gravimetric techniques; the C, N and H values were obtained using a Carbo Erba Model 1108 CHNSO elemental analyzer.

The IR spectra of polynuclear coordination compounds were recorded on KBr pellets with a JASCO FTIR 4100 spectrophotometer in the 4000–400 cm^{-1} range.

Fluorescence measurements were made with a JASCO FP 6500 and a Perkin-Elmer LS 55 spectrofluorimeters using a Xe lamp as a UV light source at ambient temperature, in the range 200-800 nm, with all the samples in solid state. The measurements were made with scan speed of 200 $nm \cdot min^{-1}$, slit of 10 nm, and cut-off filter of 1%.

UV-Vis spectra measurements were made with a JASCO V560 spectrophotometer with solid sample accessory, in the domain 200-800 nm, with a speed of 200 $nm \cdot min^{-1}$.

The thermal decomposition of the compounds was followed with a Netzsch 449C STA Jupiter. Samples were placed in open alumina crucible and heated with $10^oC\ min^{-1}$ from the room temperature to 900 ^oC, under the flow of 20 mL min^{-1} dried air.

X-ray powder diffraction patterns were obtained with a Shimadzu XRD6000 diffractometer, using Cu $K\alpha_1$ (1.5406 Å) radiation operating with 30 mA and 40 kV in the 2θ range 10–80^o. A scan rate of $1^o\ min^{-1}$ was employed.

The MB degradation was performed with 0.02 g powdered photocatalysts suspended in 50 ml solution in a Pyrex glass cell. All experiments were conducted at room temperature in air. The MB decomposition was watched with a UV–Vis spectrophotometer (JASCO V560).

3. Results and discussion

The tartarate compounds are one of the most important classes of precursors for mixed oxides. A survey of the literature shows the main types of tartarate compounds, their physico-chemical properties and thermal decomposition behaviour [16-20].

Recently, indium tartarate polymer compounds: $[In(L\text{-}TAR)H_2O] \cdot 0.5H_2O$ which contains tartarate trianions, with a 2D structure and $[In(OH)(D/L\text{-}TAR)] \cdot 2H_2O$ with 3D framework were reported [21]. Calcium tartarate tetrahydrate ($CaTAR \cdot 4H_2O$) and strontium-tartarate tetrahydrate ($SrTAR \cdot 4H_2O$) were, also, obtained [22-24]. A new coordination of a cation with the tartarate anion was put in evidence for anhydrous [Ba·TAR]. The cation exhibits ninefold coordination without the presence of water molecules. The tartarate anions are linked through Ba-O contacts, to form a tridimensional network [25].

To establish to what extent the tartarate anions can form heteropolynuclear complex compounds containing both In^{3+} and one of alkali earth (Ca^{2+}, Sr^{2+}, Ba^{2+}), the following systems have been studied:

$2In^{3+} : 1M^{2+} : 4C_4O_6H_4^{2-}$ where $M^{2+} = Ca^{2+}$, Sr^{2+}, Ba^{2+} and $C_4O_6H_4^{2-}$ = tartarate anion

The compounds of the formula were obtained:

$(NH_4)_4[CaIn_2(C_4O_6H_4)_3(OH)_6]\cdot 4H_2O$ **(I)**

$(NH_4)_3[SrIn_2(C_4O_6H_4)_3(OH)_5]\cdot 4H_2O$ **(II)**

$(NH_4)_3[BaIn_2(C_4O_6H_4)_3(OH)_5]\cdot 3H_2O$ **(III)**

These compounds have been investigated by means of infrared spectra (IR), photoluminescence spectra, simultaneous thermal analysis (TG-DSC).

3.1. Characterization of the tartarate precursors

The FTIR spectra of the compounds suggested that the tartarate anions are coordinated to metal ions through both COO^- and C-OH groups (Fig. 1). This statement is supported both by the split of the band (~ 1740 cm^{-1}) assigned to $\nu_{C=O}$ in the spectra of free tartarate acid into two very strong bands characteristic for coordinated COO^- groups $\nu_{asym}(OCO)$ ~ 1600 - 1610 $cm^{-1}$and $\nu_{sym}(OCO)$ ~ 1385 - 1390 cm^{-1} and also, by the shift towards lower frequencies (1333 - 1086 cm^{-1} $\rightarrow$ 1120 - 1075 cm^{-1}) of the bands assigned to $\nu_{(C\text{-}OH)}$.

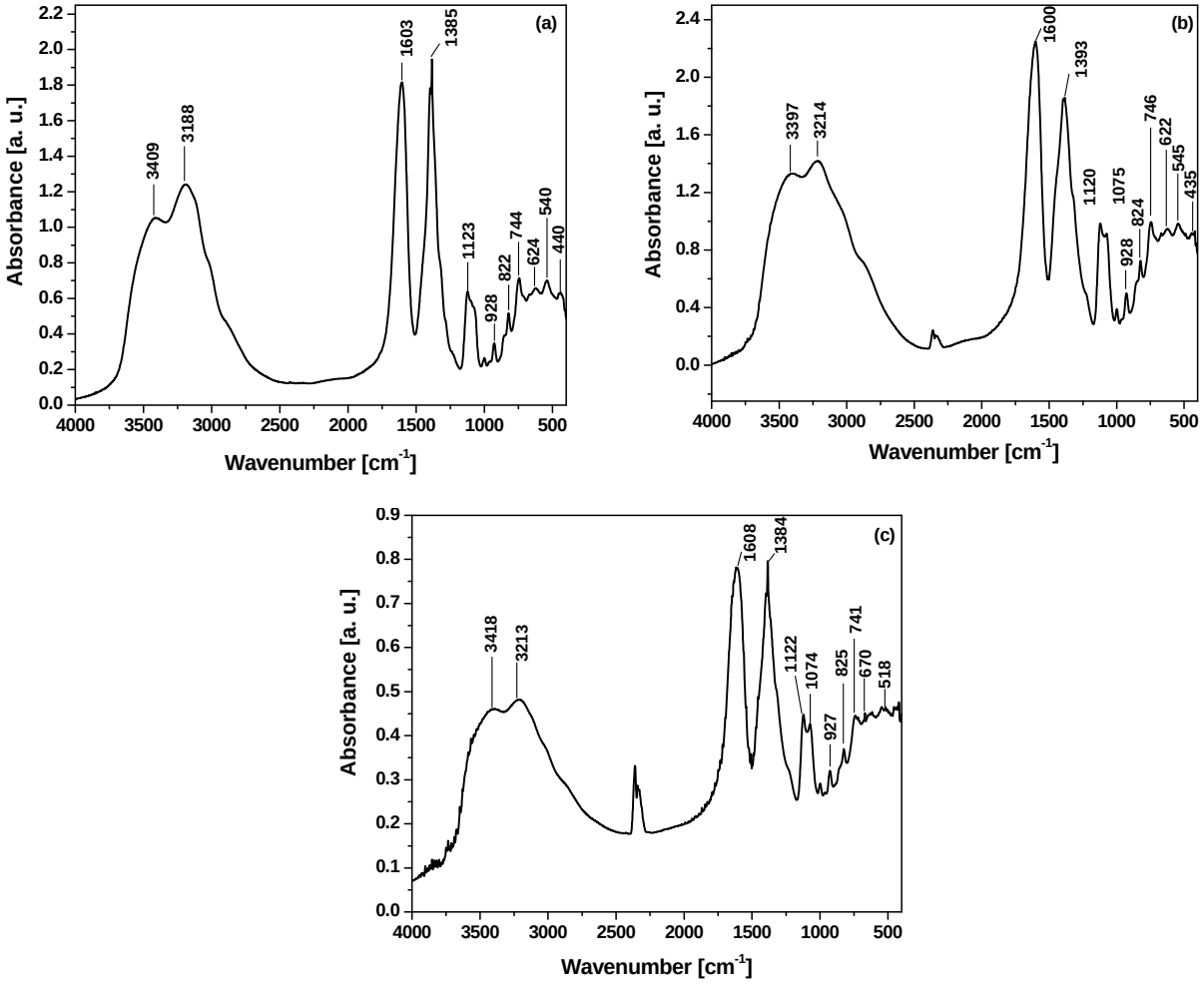

Fig. 1. IR spectra of:
(a) $(NH_4)_4[CaIn_2(C_4O_6H_4)_3(OH)_6]\cdot 4H_2O$,
(b) $(NH_4)_3[SrIn_2(C_4O_6H_4)_3(OH)_5]\cdot 4H_2O$,
(c) $(NH_4)_3[BaIn_2(C_4O_6H_4)_3(OH)_5]\cdot 3H_2O$

On the basis of spectroscopic criteria [26], the magnitude of the separation $\Delta\nu=\nu_{asym(OCO)} - \nu_{sym(OCO)}$ may be an indicative for establishing the mode of coordination of the carboxylate groups. Thus, $\Delta\nu$ values in the range 207-224 cm^{-1}, smaller than that observed for ionic compound ($\Delta\nu Na_2L$ = 240 cm^{-1}) suggested a bidentate coordination for the carboxylate groups of tartarate anions.

The FTIR spectra of indium-alkali earth tartarate compounds exhibit a broad and intense band in the 2800 – 3500 cm^{-1} range. This, band can be assigned to the vibration of water molecule/the formation of hydrogen bonds between water and/or hydroxyl groups. The presence on this band of a distinct shoulder at ~ 3160 - 3200 cm^{-1} sustains the presence of NH_4^+ groups in the molecule of tartarate compounds (Fig. 1).

The photoluminescence spectra of complex compounds were recorded with the excitation wavelength set at 320 nm (Fig. 2). The emission spectra show a broad blue emission band in the range 350 - 550 nm with a peak around 425 nm. The luminescent properties of hybrid inorganic-organic compounds are usually assigned to ligand-to-metal charge transfers (LMCT), metal-to-ligand charge transfers (MLCT), metal-centred transitions and π-π^* interligand transitions. Most probably, the emission of these compounds may originate from the ligand-to-metal charge transfer (LMCT) (since the ligand exhibits fluorescence in the range 370 - 400 nm). This process is similar to the photoluminescence of other In^{3+} carboxylate compounds reported in the literature [27, 28].

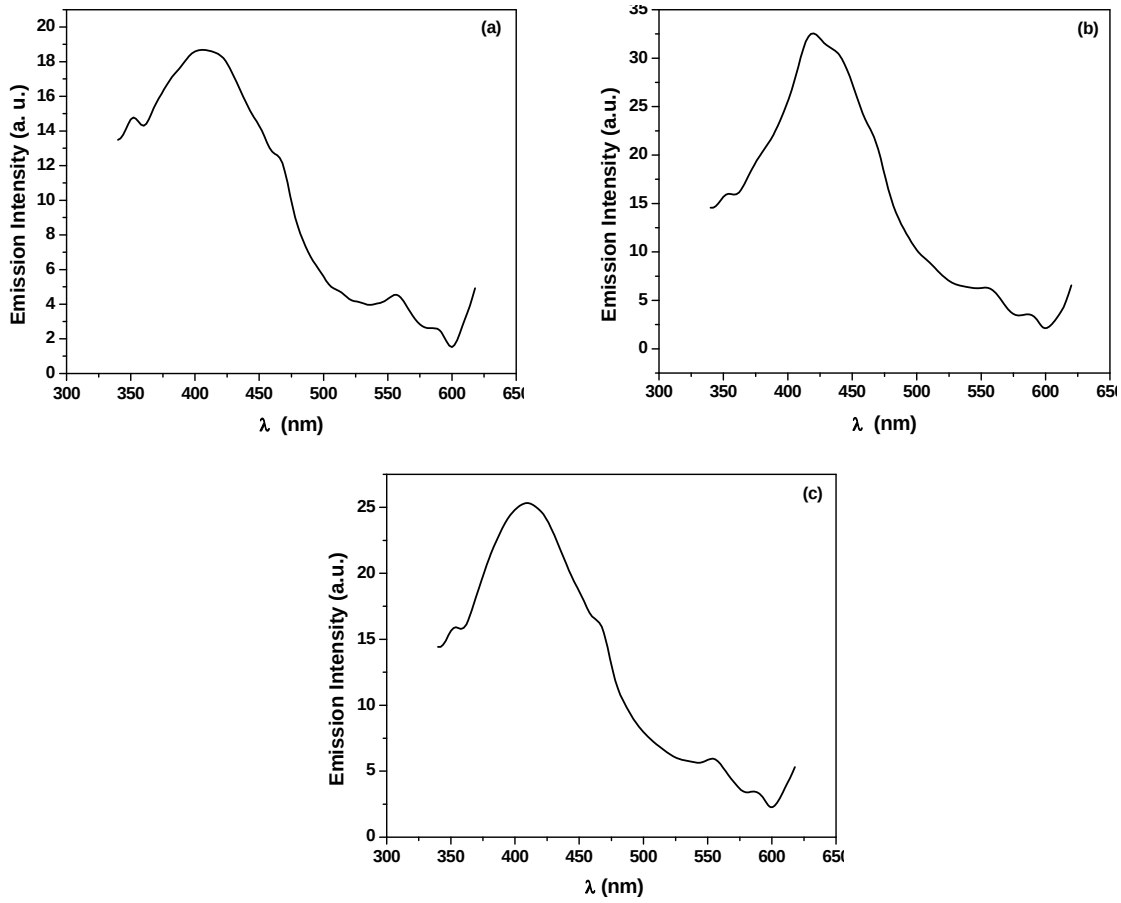

Fig. 2. Solid-state emission spectra of:
(a) $(NH_4)_4[CaIn_2(C_4O_6H_4)_3(OH)_6]\cdot 4H_2O$, (b) $(NH_4)_3[SrIn_2(C_4O_6H_4)_3(OH)_5]\cdot 4H_2O$, (c) $(NH_4)_3[BaIn_2(C_4O_6H_4)_3(OH)_5]\cdot 3H_2O$,
λ_{exc} = 320 nm

The aim of this research being the obtaining of alkali earth metal indates from these multimetallic tartarate compounds, the thermal decomposition of these compounds was investigated.

The simultaneous thermal analysis TG-DSC recorded for $(NH_4)_4[CaIn_2(C_4O_6H_4)_3(OH)_6]\cdot 4H_2O$ is presented in Fig. 3a.

The decomposition process presents two small endothermic effects in first two steps. At 326 ^oC there is a sharp, strong exothermic peak, followed by two smaller, broad peaks at 430 and 493 ^oC, which accompany the degradation of tartarate ligand to oxalate and finally to oxide [13, 15, 19, 23, 24]. The residue is formed by $CaIn_2O_4$ with traces of CaO and In_2O_3.

The simultaneous thermal analysis TG-DSC recorded for $(NH_4)_3[SrIn_2(C_4O_6H_4)_3(OH)_5]\cdot 4H_2O$ and $(NH_4)_3[BaIn_2(C_4O_6H_4)_3(OH)_5]\cdot 3H_2O$ are shown in Fig. 3b and Fig. 3c, respectively.

The decomposition pattern for compounds **II** and **III** is similar to that of compound **I**. The main observations that can be made by analyzing the TG-DSC curves are:

- the stability of compounds is very similar, but it decrease in the Ca>Sr>Ba series.
- the peaks from 166 ^oC (endo) and 430 ^oC (exo) are found only in case of compound **I**.
- the process associated with the exothermic peak from 430 ^oC seems to migrate to lower temperatures from Ca to Sr and Ba (the effect being present as a shoulder near the main sharp exothermic peak).
- the last process (the decomposition of carbonate anion) takes place at an increasing temperature in the series Ca<Sr<Ba, as it was expected from corresponding pure carbonates.

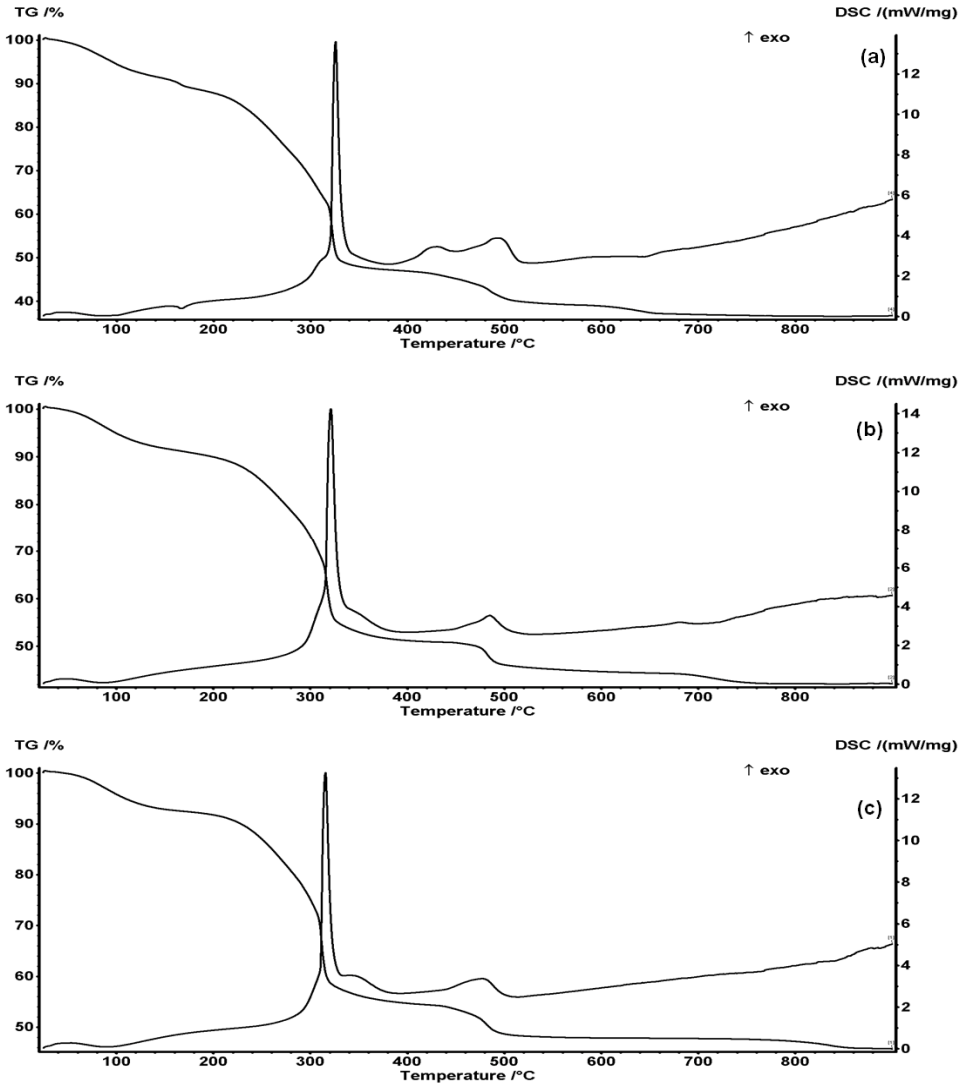

Fig. 3. TG and DSC curves for: (a) $(NH_4)_4[CaIn_2(C_4O_6H_4)_3(OH)_6]\cdot 4H_2O$, (b) $(NH_4)_3[SrIn_2(C_4O_6H_4)_3(OH)_5]\cdot 4H_2O$, (c) $(NH_4)_3[BaIn_2(C_4O_6H_4)_3(OH)_5]\cdot 3H_2O$

The TG data for all compounds are presented in Table 1, together with the proposed decomposition pathway.

*Table1. TG data for compounds **I, II** and **III***

Compd	Step	Temp. int. [°C]	Exp. weight loss [%]	Cal. weight loss [%]	Observations
I	1	40-180	11.19	11.14	Loss of 4 crystallization H_2O molecules, one NH_3 molecule and one OH from coordination sphere as H_2O
	2	180-317	26.27	26.97	Loss of 3 NH_3 molecules and 5 OH from coordination sphere as H_2O. Ligand decomposition
	3	317-380	15.37	14.99	Loss of 2 CO_2 and 2 CO molecules
	4	380-530	7.57	7.49	Loss of one CO_2 and one CO molecules
	5	530-900	3.02	4.58	Decomposition of carbonate ion
II	1	40-180	9.30	9.15	Loss of 4 crystallization H_2O molecules and one NH_3 molecule
	2	180-312	22.43	22.00	Loss of 2 NH_3 molecules and OH from coordination sphere as H_2O. Ligand decomposition
	3	312-410	17.25	17.68	Loss of 2 CO_2 and 3 CO molecules
	4	410-530	5.61	7.40	Loss of one CO_2 and one CO molecules
	5	530-900	3.29	4.52	Decomposition of carbonate ion
III	1	40-170	7.60	7.07	Loss of 3 crystallization H_2O molecules and one NH_3 molecule
	2	170-305	19.12	21.30	Loss of 2 NH_3 molecules and OH from coordination sphere as H_2O. Ligand decomposition
	3	305-395	18.53	17.12	Loss of 2 CO_2 and 3 CO molecules
	4	395-515	6.48	7.16	Loss of one CO_2 and one CO molecules
	5	515-900	2.57	4.38	Partial decomposition of carbonate ion

3.2. Characterization of the alkali earth metal indates

It is well known that $CaIn_2O_4$ and $SrIn_2O_4$ have similar crystal structure different from $BaIn_2O_4$ [2, 8, 29, 30]. The structures of $CaIn_2O_4$ and $SrIn_2O_4$ are isostructural to $CaFe_2O_4$ and belong to the orthorhombic system, space group Pnam (orthorhombic phase of $CaIn_2O_4$ (ICDD 17-0643); orthorhombic phase of $SrIn_2O_4$ (ICDD 33-1336)). $BaIn_2O_4$ has a monoclinic structure, space group P21/a (ICDD 35-1064), isostructural with other monoclinic AB_2O_4 compounds such as $SrAl_2O_4$ [31-33].

The XRD pattern of the $CaIn_2O_4$ sample obtained at 900°C is shown in Fig. 4a. The $CaIn_2O_4$ with orthorhombic structure was obtained together with traces of In_2O_3 and CaO.

The crystallite size of the samples can be estimated from the Scherrer equation ($D = 0.89 \cdot \lambda/\beta \cdot \cos\theta$, where D is the average grain size, λ is the X-ray wavelength (0.15405 nm), θ and β are the diffraction angle and FWHM of an observed peak, respectively [30]). The strongest peak (121) at $2\theta = 33.44^o$ was used to calculate the average crystallite size (D) of $CaIn_2O_4$ particles. The

estimated average crystallite size is about 32.7 nm. We have also calculated the crystallite size for In_2O_3 using the strongest peak (222) at $2\theta = 30.63^o$, obtaining an average size of about 37 nm.

The XRD pattern of the $SrIn_2O_4$ sample obtained at 900 ^oC is shown in Fig. 4b. The $SrIn_2O_4$ with orthorhombic structure was obtained together with traces of In_2O_3 and SrO. The strongest peak (201) at $2\theta = 32.83^o$ was used to calculate the average crystallite size of $SrIn_2O_4$ particles. The estimated average crystallite size is about 25 nm. We have also calculated the crystallite size for In_2O_3 using the strongest peak (222) at $2\theta = 30.58^o$, obtaining an average size of about 26 nm.

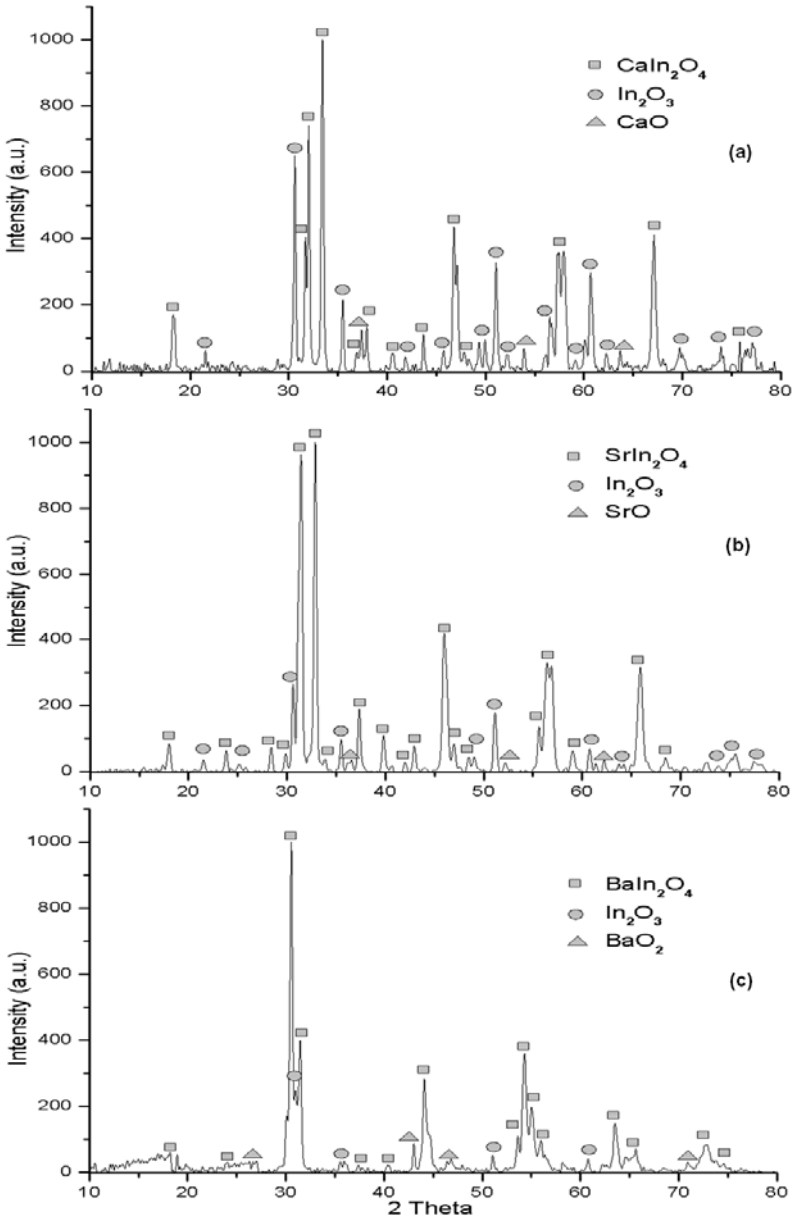

Fig. 4. *The XRD pattern of:*
(a) $CaIn_2O_4$ obtain by decomposition of $(NH_4)_4[CaIn_2(C_4O_6H_4)_3(OH)_6]\cdot 4H_2O$, (b) $SrIn_2O_4$ obtain by decomposition of $(NH_4)_3[SrIn_2(C_4O_6H_4)_3(OH)_5]\cdot 4H_2O$, (c) $BaIn_2O_4$ obtain by decomposition of $(NH_4)_3[BaIn_2(C_4O_6H_4)_3(OH)_5]\cdot 3H_2O$ and treated at 1100 °C

The sample obtained at 900 ^oC did not presented the XRD pattern characteristic for $BaIn_2O_4$. In order to obtain $BaIn_2O_4$, we have increased the temperature of thermal treatment to 1100 ^oC. The XRD pattern of the $BaIn_2O_4$ sample obtained at 1100 ^oC is shown in Fig. 4c. The $BaIn_2O_4$ with monoclinic structure was obtained together with traces of In_2O_3 and BaO_2. The

strongest peak (031) at 2θ = 31.48° was used to calculate the average crystallite size of $BaIn_2O_4$ particles. The estimated average crystallite size is about 21 nm.

The IR spectra of these oxides revealed the stretching vibrations of the InO_6 octahedron ν(InO_6) in the range 440-600 cm^{-1} [29]. Fig. 5 presents the IR spectrum recorded for $CaIn_2O_4$ in 440 - 1000 cm^{-1} range.

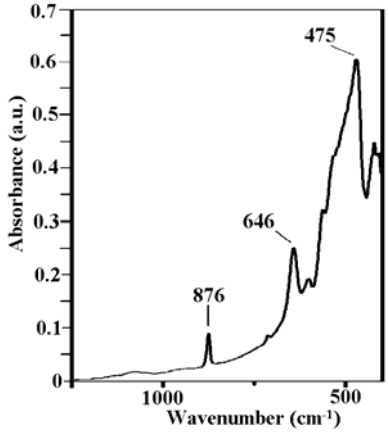

Fig. 5. IR spectrum of $CaIn_2O_4$ obtain by calcination of $(NH_4)_4[CaIn_2(C_4O_6H_4)_3(OH)_6]\cdot 4H_2O$

The diffuse reflectance spectra of these indates are recorded between 200 - 800 nm (Fig. 6). The strong absorptions bands around 260 - 400 nm are due to the electron transition from valence bands (VB) (consisting of the 2p orbital of O) to the conduction bands (CBs) (consisting of the 5s and 5p indium orbitals) [2, 29].

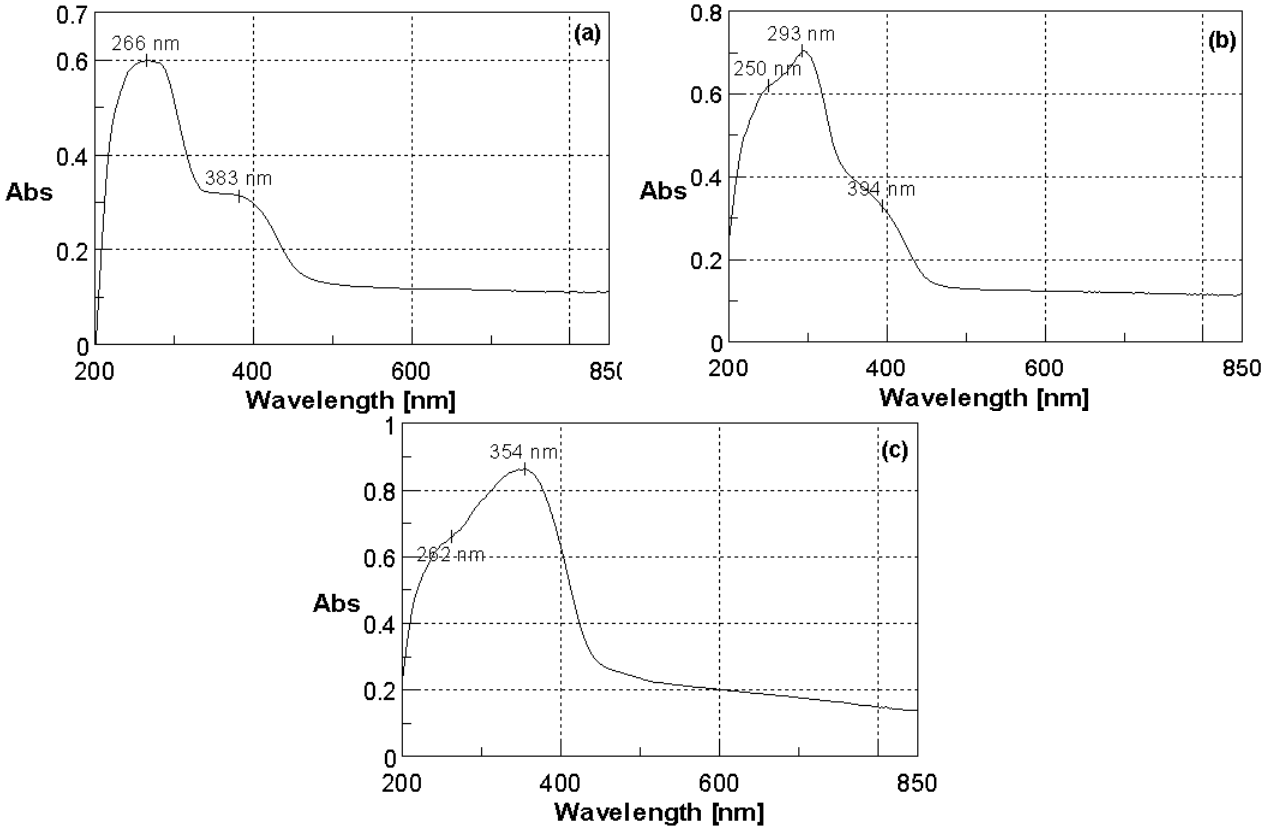

Fig. 6. Diffuse reflectance spectra of:
(a) $CaIn_2O_4$ obtain by decomposition of $(NH_4)_4[CaIn_2(C_4O_6H_4)_3(OH)_6]\cdot 4H_2O$ at 900°C,
(b) $SrIn_2O_4$ obtain by decomposition of $(NH_4)_3[SrIn_2(C_4O_6H_4)_3(OH)_5]\cdot 4H_2O$ at 900°C,
(c) $BaIn_2O_4$ obtain by decomposition of $(NH_4)_3[BaIn_2(C_4O_6H_4)_3(OH)_5]\cdot 3H_2O$ at 1100 ℃

The diffuse reflectance spectra permitted us to estimate the value of the band gap in the MIn_2O_4 sample. The calculated values are: 3.86 eV, 3.75 eV, 3.31 eV for $CaIn_2O_4$, $SrIn_2O_4$ and $BaIn_2O_4$ respectively, in good agreement with the literature [7].

In order to identify the origin of the weak blue emission band of MIn_2O_4 (M^{2+}=Ca^{2+}, Sr^{2+}, Ba^{2+}) the emission spectra of these indates were recorded using the same excitation conditions (374 nm) [30, 31, 33-36]

Fig. 7 shows the excitation and emission spectra of the $CaIn_2O_4$ sample.

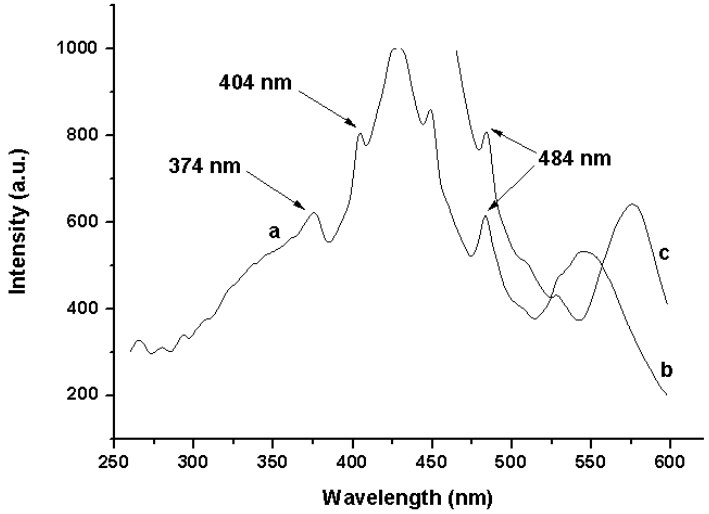

Fig. 7. Excitation and emission spectra of the $CaIn_2O_4$ sample: (a) excitation spectra for 484 nm emission, (b) emission spectra for 374 nm excitation, (c) emission spectra for 404 nm excitation

The excitation spectrum of the $CaIn_2O_4$ sample monitored with 484 nm emission (Fig.7a) consists of a strong excitation band from 260 to 420 nm with a maximum at 404 nm and some weaker lines (265, 280, 294, 309, 374 nm) in the shorter wavelength region. Under 374 or 404 nm excitation, the $CaIn_2O_4$ sample shows a strong blue luminescence. The emission spectrum (Fig. 7b and 7c) of $CaIn_2O_4$ sample consists of a strong blue emission band ranging from 440 to 600 nm, with a maximum at 484 nm. The blue emission of $CaIn_2O_4$ sample can be attributed to the recombination of an electron on a donor formed by oxygen vacancies with a hole on an acceptor consisting of either calcium vacancies or indium vacancies [30].

Fig. 8 and Fig. 9 show the excitation and emission spectra of the $SrIn_2O_4$ and $BaIn_2O_4$ samples.

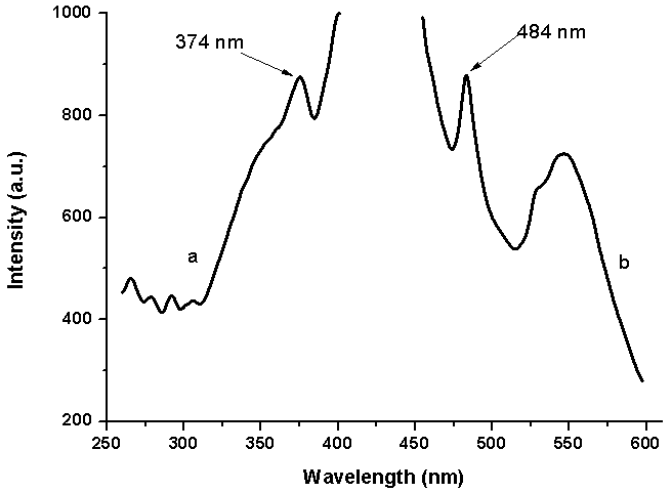

Fig. 8. Excitation and emission spectra of the $SrIn_2O_4$ sample: (a) excitation spectra for 484 nm emission, (b) emission spectra for 374 nm excitation

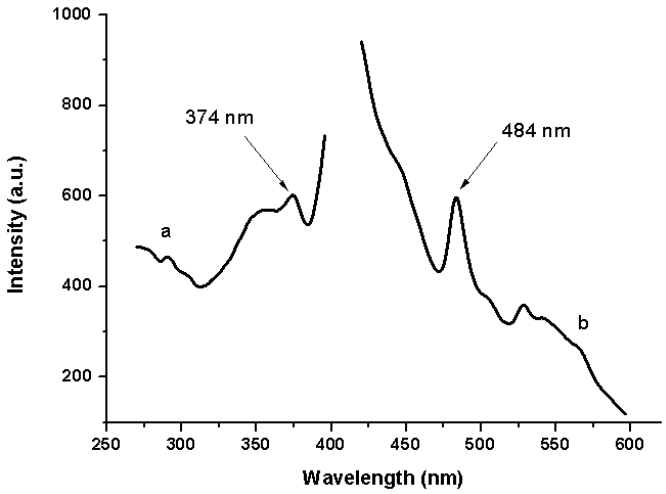

Fig. 9. Excitation and emission spectra of the $BaIn_2O_4$ sample: (a) excitation spectra for 484 nm emission; (b) emission spectra for 374 nm excitation

The spectra have the same shape as the $CaIn_2O_4$, suggesting the same formation mechanism. The intensity of the excitation and emission bands is higher in the case of $SrIn_2O_4$ than in the case of $CaIn_2O_4$ and $BaIn_2O_4$ indicating a better fluorescence output (Fig. 8).

A simple model illustrating the blue emission process in MIn_2O_4 is shown in Fig. 10.

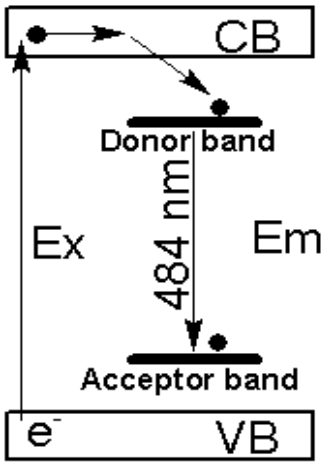

Fig. 10. Proposed simple model illustrating the blue emission process in MIn_2O_4 (M = Ca, Sr, Ba).

Under the excitation of a 374 nm irradiation (bandgap excitation), an electron (*) is excited from the VB to the CB. The electron (*) moves freely around the CB and finally relaxes to the donor band (oxygen vacancies). The recombination of the electron in the donor band with the acceptor (alkali-earth vacancies or indium vacancies) yields a blue emission with a maximum wavelength at 484 nm [30].

The photocatalytic activity was measured against Methylene blue (MB) (which is often used as model dye contaminant to evaluate the activity of a photocatalyst), Fig. 11.

We found a good photocatalytic activity for $CaIn_2O_4$, in good agreement with the literature [2]. Nevertheless in the case of $SrIn_2O_4$ and $BaIn_2O_4$ the absorbance spectra was identical with that of the control sample (the cell containing only MB solution), indicating no photocatalytic activity despite some earlier reports [2].

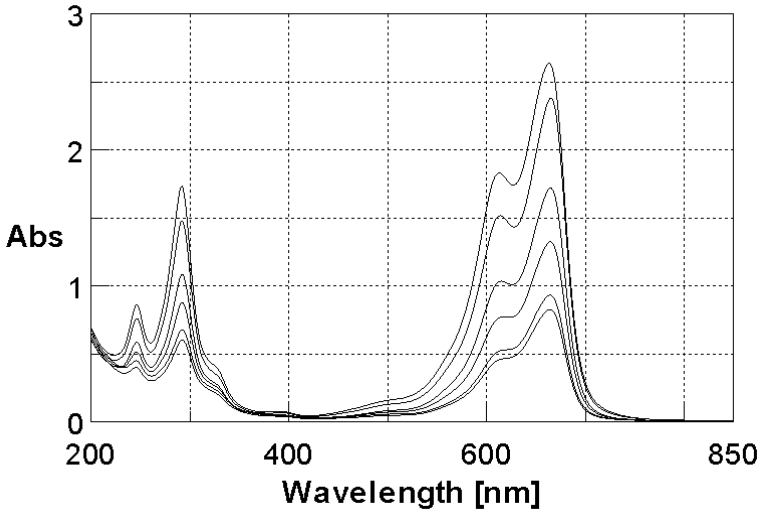

Fig. 11. The photocatalytic activity of $CaIn_2O_4$ – MB spectra measured at T0 and from 2 to 2 hours after T0.

4. Conclusion

The precursor method – *via* tartarate route was favourable for obtaining nanostructured $CaIn_2O_4$/$SrIn_2O_4$ with orthorhombic structure and $BaIn_2O_4$ with monoclinic structure. The average crystallite size varied between 21 - 33 nm. The emission spectra of indates evidenced a strong blue emission band ranging from 440 - 600 nm, with a maximum at ~ 484 nm. $CaIn_2O_4$ had a good photocatalytic activity in agreement with literature data.

Acknowledgments

This work was supported by the programme "Coordination and supramolecular chemistry" of the "Ilie Murgulescu" Institute of Physical Chemistry, financed by the Romanian Academy and by the research program CNCSIS –UEFISCSU PNII – IDEI 1364/2008.

References

[1] J. W. Tang, Z. G. Zou, J. H. Ye, Chem. Phys. Lett. **382,** 175 (2003).
[2] J. W. Tang, Z. G. Zou, M. Katagiri, T. Kato, J. H. Ye, Catal. Today **93-95**, 885 (2004).
[3] J. W. Tang, Z. G. Zou, J. H. Ye, Chem. Mater. **16,** 1644 (2004).
[4] J. Sato, H. Kobayashi, Y. Inoue, J. Phys. Chem. B **107,** 7970 (2003).
[5] J. Sato, H. Kobayashi, Y. Inoue, J. Phys. Chem. B **107**, 7965 (2003).
[6] F. R. Cruickshank, D. McK Taylor, P. F. Glasser, J. Inorg. Nucl. Chem. **26,** 937 (1964).
[7] E. S. Dali, V. V. S. S. Sai Sundar, M. Jayachandran, M. J. Chockalingam, J. Mater. Sci. Lett. **17,** 619 (1998).
[8] J. Ding, S. Sun, J. Bao, Z. Luo, Ch. Gao, Catal. Lett. **130**, 147 (2009).
[9] S. P. Khatkar, V. B. Tascak, S. D. Han, J. Y. Park, D. Kumar, Mater. Chem. Phys. **98,** 528 (2006).
[10] I. Mindru, G. Marinescu, D. Gingasu, L. Patron, L. Diamandescu, C. Ghica, B. Mironov, Mat. Sci. Eng. B **170,** 99 (2010).
[11] I. Mindru, G. Marinescu, D. Gingasu, L. Patron, C. Ghica, M. Giurginca, Mater. Chem. Phys. **122,** 491 (2010).
[12] D. Gingasu, I. Mindru. G. Marinescu, L. Patron, C. Ghica, J. Alloys Compd. **481,** 890 (2009).
[13] D. Gingasu, I. Mindru, L. Patron, S. Stoleriu, J Serb. Chem. Soc **73,** 979 (2008).
[14] C. Suciu**,** I. Mindru, G. Marinescu , O. Carp, L. Patron, J Optoelectron Adv. Mater. **10,** 1452 (2008).

[15] O. Carp, L. Patron, I. Mindru, C. Suciu, J. Therm. Anal. Calorim. **881,** 77 (2007).
[16] E.C. Rodriguez, C.J. Carvalho, A.B de Siqueira, G. Bannach, M. Ionashiro, Thermochim. Acta **496,** 156 (2009).
[17] R.M. Sharma, M.J. Kaul, J. Indian Chem. **67,** 706 (1990).
[18] N. Deb, J. Therm. Anal. Calorim. **78**, 227 (2004).
[19] K.K. Bamzai, S. Kumar, Mater. Chem. Phys. **107**, 200 (2008).
[20] N.N. Dass, S. Sarmah, J. Therm. Anal. Calorim. **58**, 137 (1999).
[21] A.S. –F. Au-Yeung, H. H.-Y. Sung, J.A.K. Cha, A.W.-H. Siu, S.S. Chui, I.D. Williams, Inorg. Chem. Commun. **9**, 507 (2006).
[22] P.P. Pradyumnan, C. Shini, Indian J. Pure Ap. Phy. **47**, 199 (2009).
[23] S.K. Arora, V. Patel, A. Kothari, Mater. Chem. Phys. **84,** 323 (2004).
[24] M.H. Rahimkutty, K.R.Babu, K.S. Pillai, M.R.S. Kumar, C.M.K. Nair, Bull. Mater. Sci. **24**, 249 (2001).
[25] C. Gonzalez-Silgo, J. Gonzalez-Platas, C. Ruiz-Perez, T. Lopez, M. Torres, Acta Crystallogr. C **55** 740 (1999).
[26] K. Nakamoto, Infrared and Raman Spectra of Inorganic and Coordination Compounds, Wiley, New York (1986).
[27] Z.Z. Lin, L. Cheng, F. L. Jing, Inorg. Chem. Commun. **8**, 199 (2005).
[28] C. Jun-Jun, G.-D. Li, C. Jie-Sheng, J. Solid State Chem. **182**, 102 (2009).
[29] A. Baszczuk, M. Jasiorski, M. Nyk, J. Ibanuza, M. Maczka, W. Strek, J. Alloys Compd. **394**, 88 (2005).
[30] X. Liu, R. Panga, Q. Li, J. Lin, J Solid State Chem. **180**, 1421 (2007).
[31] H. Deng, Q. Wang, P. Ren, J. Wu, J. Tao, X. Chen, N. Dai, Chinese Opt. Lett. **9**, 011602(1) (2011).
[32] P. Escribano, H. Marchal, M.L. Sanjuan, P. Gutierez, B. Julian, E. Cordoncello, J. Solid State Chem. **178**, 1978 (2005).
[33] F. Clabau, X. Rocquefelte, S. Jobic, P. Deniard, M.H. Whangbo, A. Garcia, T. Le Mercier, Solid State Sci. **9**, 608 (2007).
[34] W.Y. Shen, H.L. Pang, J. Lin, J. Fang, J. Electrochem. Soc. **152**, H25 (2005).
[35] D. Bai, Z. Zhang, L. Li, F. Xu, K. Yu, Cryst. Res. Technol. **45**, 173 (2010).
[36] C.Q. Wang, D.R. Chen, X.L. Liao, J. Phys. Chem. C **113**, 7714 (2009).